10µm Backside Illuminated SPAD cell with Novel Dielectric-Filled DTI Scheme for optical Isolation

Becky Lavi
Tower Semiconductor
Shaul Amor 20, Migdal Haaemek, Israel
beckila@towersemi.com

Adi Birman
Tower Semiconductor
Shaul Amor 20, Migdal Haaemek, Israel
adibi@towersemi.com

Dmitry Veinger
Tower Semiconductor
Shaul Amor 20, Migdal Haaemek, Israel
dmitry.veinger@towersemi.com

Nobuyoshi Takahashi
Tower Partner Semiconductor Co. Ltd. 800 Higashiyama, Uozu City, Toyama, Japan
takahashi.nobuyoshi@tpsemico.com

Shirly Regev
Etesian Semiconductor Ltd
P.O.B 3227, Ramat Yishai, Israel
shirly.regev@etesiansemi.com

Amos Fenigstein
Tower Semiconductor
Shaul Amor 20, Migdal Haaemek, Israel
amosfe@towersemi.com

***Abstract* — We present a 10.5µm back-side illuminated 3D-stacked single-photon avalanche diode (SPAD) sensor with reduced crosstalk and improved photon detection efficiency (PDE) performance. To minimize crosstalk, we employ an innovative double Deep Trench Isolation (DTI) solution. Enhanced PDE is achieved by optimizing the SPAD implant process to focus the generated carriers from the entire pixel volume into the high field avalanche region near the SPAD junction.**

Keywords — SPAD, Crosstalk, PDE, DTI

I. INTRODUCTION

Arrays of Single Photon Avalanche Photodiodes (SPADs) are the heart of Direct Time of Flight (DToF) sensors for distance mapping [1]. These photodiodes operate in Geiger mode; when charged to a specific Excess Voltage (V_{EB}) above the Breakdown Voltage (V_{BD}), they undergo an avalanche upon photon impact. Such sensors are used for a large range of applications, from face recognition in cell phones to vacuum cleaners and automotive LiDAR systems.

Over the past decade, interest in SPADs has been growing significantly, leading to remarkable advancements in their performance [2]. To optimize high-performing DToF sensors based on SPAD matrices, several key performance parameters must be considered [3], [4]. High Photon Detection Efficiency (PDE), defined as the percentage of photons impinging on the pixel causing avalanche is a critical factor. Since the wavelengths of the illuminating lasers typically range from 900 to 940 nm, optimizing PDE for these wavelengths is essential. Other important parameters include a low Dark Count Rate (DCR), which measures the rate of avalanche events per second in the absence of illumination, and minimal crosstalk, which refers to the probability of avalanche events occurring in neighboring pixels compared to the one directly hit by a photon. All these should be achieved with relatively low V_{EB} to ensure compatibility with operating circuits.

For LiDAR applications, particularly in the automotive LiDAR's, a large-format SPAD image sensor is required. Thus, the scaling down of a SPAD cell to smaller pitches is crucial. This need has driven the development of SPAD cells using deep submicron CMOS technologies, ranging from 180nm down to 40nm [3]. The incorporation of backside illumination (BSI) and 3D stacking technologies enables the integration of sophisticated CMOS logic circuitry within a compact pixel layout [5].

However, minimizing the SPAD cell presents challenges in maintaining high PDE values while also minimizing crosstalk, which tends to increase with smaller pixel pitches. Recent studies have introduced various methods to enhance PDE in small SPAD cells [2], [6], [7], including light scattering structures and charge focusing diodes. To address the issue of crosstalk, deep trench isolation (DTI) has been implemented between pixels. To a certain extent, crosstalk can be managed through the application of correction algorithms [8].

In this work, we present a 10.5µm SPAD cell that demonstrates improved PDE at 940nm while also reducing crosstalk.

II. SPAD CELL STREUCTURE

Figure 1 illustrates the basic structure of the SPAD cell: a 10.5µm pitch, 3D-stacked BSI sensor. It is manufactured with a 65nm technology on a 6µm thick Si and equipped with dielectric filled DTI at four borders, along with light scattering structures on its backside. Additionally, a metal reflector is positioned beneath the diode's active area, opposite to incoming light direction. All these together create a "light trapping" mechanism that extends the light path through the cell volume, thereby PDE.

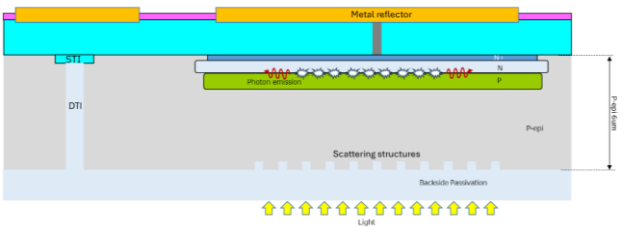

Fig. 1. – A 10.5 µm pitch backside-illuminated SPAD cell featuring Deep Trench Isolation (DTI) and a light scattering structure on its backside. A metal reflector is positioned beneath the diode's active area, opposite to the direction of incoming light.

III. Crosstalk in SPAD Array

The primary mechanism of crosstalk in SPAD arrays arises from the emission of near-infrared (NIR) and visible photons generated by avalanche events. These photons can penetrate neighboring SPADs, leading to secondary avalanche events in those adjacent cells. Naturally, SPAD cell miniaturization leads to enhanced photon emission crosstalk. Since the conventional DTI is filled with transparent dielectric material, it is ineffective at blocking these emitted photons. In this work, we propose a solution using double and triple fragmented DTI lines. This approach is based on the phenomenon of total internal reflection at the dielectric interface for angles exceeding the critical angle (20.1° for the Si/SiO2 interface at visible light). Figure 2a presents three examples of the double and triple fragmented DTI lines: a.1 shows a straight trench parallel to a series of tilted small trenches; a.2 depicts two parallel series of tilted small trenches; and a.3 illustrates a straight trench edged by two parallel series of tilted small trenches on either side. These DTI fragments are strategically arranged so that any photon, regardless of its trajectory, will encounter total internal reflection at least once, as demonstrated in Figure 2b.

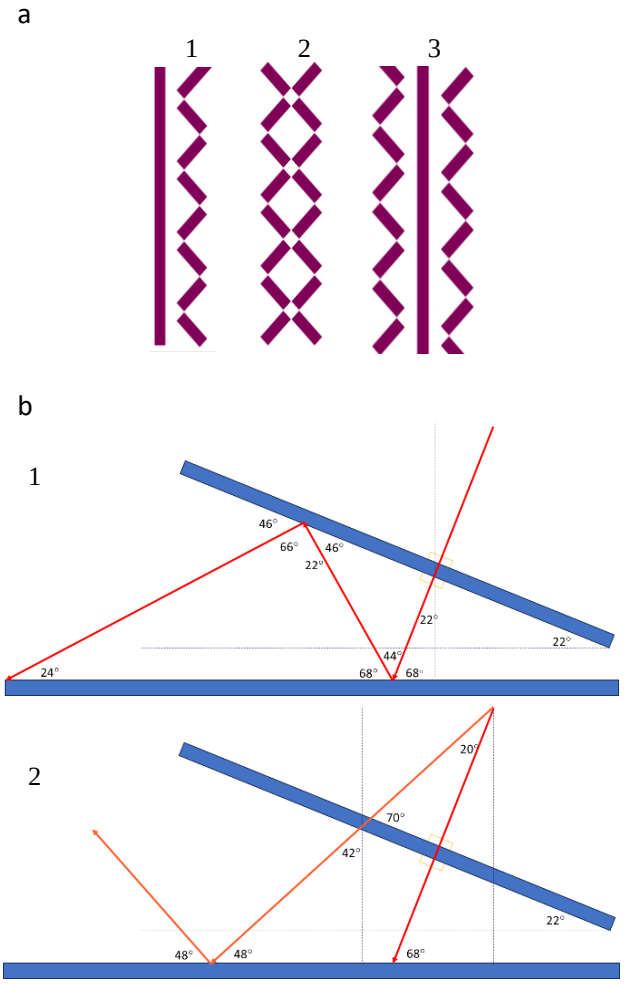

Fig. 2. – a) segments of different DTI arrangements: 1. straight trench parallel to a series of tilted small trenches; 2. two parallel series of tilted small trenches; 3. straight trench edged by two parallel series of tilted small trenches on either side. b) 2 examples of photons hitting the tilted DTI with angles of 0° (1) and 20° (2). In both scenarios, the photon will reflect off the straight DTI since the angle relative to the straight DTI exceeds the critical angle.

The optical simulations illustrating the response of a pixel to photons emitted from a neighboring pixel are shown in Figure 3. The left image depicts the standard single DTI configuration, while the right image presents the double DTI scheme.

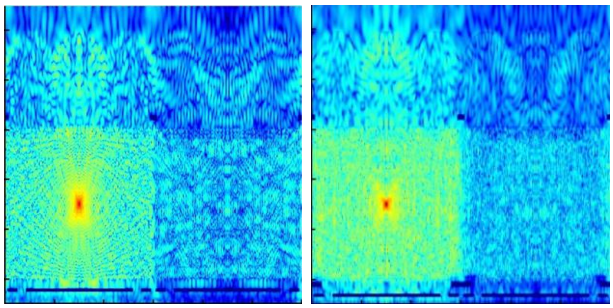

Fig. 3. – Optical simulation showing the response of a cell to photons emitted from a neighboring cell. The left image represents the standard single DTI scheme, while the right image illustrates the double DTI scheme.

As illustrated in Figure 4, the double DTI scheme (shown in Figure 2a.1) results in crosstalk levels that are less than half those measured with the single DTI scheme. These crosstalk values were obtained from a diode structure as demonstrated in Figure 1.

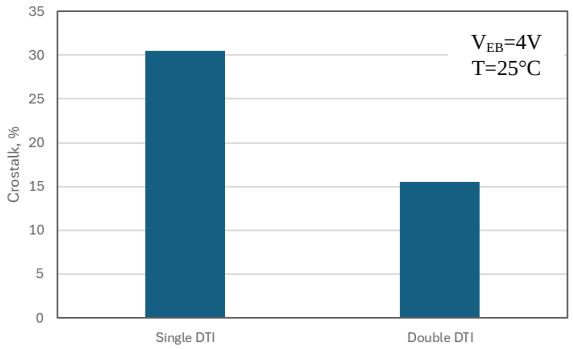

Fig. 4. – Measured crosstalk of different DTI schemes; single DTI versus double DTI.

IV. PDE Enhancement

The double and triple DTI configurations consume a significant area of the pixel, leading to a reduced fill factor and consequently a decrease in PDE. To overcome this loss in PDE, it is essential to optimize the implant scheme of the SPAD to effectively direct the generated carriers from the entire pixel volume into the multiplication region near the SPAD junction (a charge focusing scheme). Figure 5 illustrates a simulation of this implant scheme, demonstrating how the electric field guides the electrons into the volume with a high probability of avalanche breakdown.

The improved process concept proposed by the TCAD simulation, along with the described double DTI scheme, was implemented in a SPAD cell and processed with a 65nm technology. The results, presented in Table 1, compare the performance of a standard SPAD cell that employs a single DTI and a conventional diode scheme with that of the improved SPAD cell that utilizes double DTI and a charge-focusing implantation scheme. The resultant PDE and cross-talk were significantly improved

all while maintaining a relatively low V_{EB} of less than 2.0V. The PDE values presented in Table 1 were obtained from a SPAD cell without a microlens. Based on prior observations, conventional SPAD cells demonstrate a typical PDE enhancement of 30-40% upon microlens application. We predict smaller PDE improvement for our enhanced SPAD cell. Nonetheless, a positive PDE gain is expected upon microlens application.

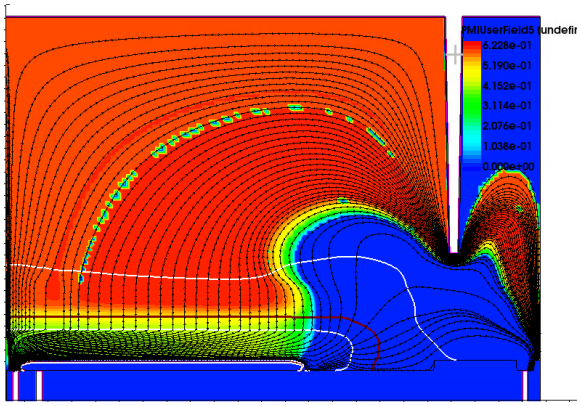

Fig. 5. – TCAD simulation of the optimized implantation scheme, demonstrating carrier transport to the avalanche region in a near the junction of the SAPD. Electric field streamlines show the electron flow towards the multiplication area. Color coding represents the probability of an electron, generated at a given location, reaching the multiplication area and initiating an avalanche event.

TABLE I. A COMPARISON OF THE PERFORMANCE OF A SPAD CELL WITH A SINGLE DTI AND A CONVENTIONAL DIODE SCHEME (FIGURE 1) VERSUS THE IMPROVED SPAD CELLS FEATURING DOUBLE DTI AND A CHARGE-FOCUSING IMPLANTATION SCHEME.

SPAD cell concept	PDE*, %	DCR, cps	XT, %	V_{EB}, V
Single DTI and conventional diode scheme	10	83	30	4
Double DTI with charge focusing diode scheme	21.5	140	9	1.3

* Measured at 940nm and 25°C **without** microlens

V. CONCLUSION

A BSI 3D-stacked 10.5µm SPAD cell has been developed, achieving a PDE exceeding 20% at a wavelength of 940nm, with crosstalk remaining below 10%. It has been shown that a SPAD pixel with transparent DTI can be optimized to achieve reduced crosstalk preserving high PDE and enabling low overvoltage operation. This optimization is achieved with a tolerable increase in DCR.

REFERENCES

[1] M. Wojtkiewicz and R. K. Henderson, "Review of Back-Side Illuminated 3-D-Stacked SPADs for Time-of-Flight and Single-Photon Imaging", IEEE transactions on electron devices, vol. 71, no. 6, pp. 3470-3477, June 2024.

[2] Y. Fujisaki, H. Tsugawa, K. Sakai, H. Kumagai, R. Nakamura, T. Ogita, "A back-illuminated 6 µm SPAD depth sensor with PDE 36.5% at 940 nm via combination of dual diffraction structure and 2×2 on-chip lens", Symposium on VLSI Technology, June 2023

[3] E. Charbon, "SPAD Image Sensors for Quantum and Classical Imaging", STO Meetings proceedings, January 2024.

[4] D. Bronzi, F. Villa, S. Tisa, A. Tosi, F. Zappa, "SPAD Figures of Merit for Photon-Counting, Photon-Timing, and Imaging Applications: A Review", IEEE Sensors Journal, vol. 16, no. 1, pp. 3-12, January 2016.

[5] J. Ogi, S. Kitamura, F. Sugaya, J. Suzuki, A. Magori, T. Matsui, K. Sumita, Y. Ushiku, K. Moriyama, K. Toshima, T. Namise, H. Ozawa, Y. Tsukuda, Y. Otake, H. Hiyama, S. Matsumoto, A. Suzuki, F. Koga, "A 2.1-ns Dead Time 5-µm Single Photon Avalanche Diode with 2-layer Transistor Pixel Technology", IEEE International Electron Devices Meeting (IEDM), December 2024.

[6] K. Morimoto, J. Iwata, M. Shinohara, H. Sekine, A. Abdelghafar, H. Tsuchiya, Y. Kuroda, K. Tojima, W. Endo, Y. Maehashi, Y. Ota, T. Sasago, S. Maekawa, S. Hikosaka, T. Kanou, A. Kato, T. Tezuka, S. Yoshizaki, T. Ogawa, K. Uehira, A. Ehara, F. Inui, Y. Matsuno, K. Sakurai, T. Ichikawa, "3.2 Megapixel 3D-Stacked Charge Focusing SPAD for Low-Light Imaging and Depth Sensing", IEEE International Electron Devices Meeting (IEDM), December 2021.

[7] B. Mamdy, R. A. Bianchi, D. Golanski, B. Rae, T. M. Bah, D. Rideau, F. Twaddle, R. Helleboid, C. Buj, N. Moussy, R. Fillon, Y. Henrion, E. Lacombe, R. Neri, F. Brun, I. Nicholson, M. Agnew, B. Murray, M. Basset, R. Perrier, M. Al-Rawhani, S. Jouan, A. Lopez, L. Stark, S. Pellegrini, "A high PDE and high maximum count rate and low power consumption 3D-stacked SPAD device for Lidar applications", International Image Sensor Workshop, May 2023.

[8] A. Abdelghafar, K. Morimoto, H. Sekine, H. Tsuchiya, M. Shinohara, Y. Ota, J. Iwata, Y. Matsuno, K. Sakurai, and T. Ichikawa, "Light-Emission Crosstalk Model and Dynamic Correction Algorithm for Large-Scale SPAD Image Sensors", International Image Sensor Workshop, May 2023.